Frontiers in Life Sciences and Related Technologies 3(3) (2022) 101-106

Contents lists available at Dergipark

Frontiers in Life Sciences and Related Technologies

Journal homepage: http://dergipark.org.tr/en/pub/flsrt

Research article

Determination of optical constants and band gap variation of $Zn_{0.98-x}Cu_{0.02}Mg_xO$ thin films

Dogan Akcan*[1]

[1] *Bahcesehir University, Faculty of Engineering and Natural Sciences, Department of Mathematics, 34353, Istanbul, Türkiye*

Abstract

Cu doped ZnO ($ZnCuO$) is a very important candidate for electronic applications, since it has been shown that it possesses p–type conductivity. In order to broaden its applications, it is crucial to tune optical and electronic properties. In this study, by doping $ZnCuO$ with magnesium, variation of refractive index, extinction coefficient, and band gap of thin films were investigated. Optical constants were evaluated using a transmittance model which is derived from Fresnel equations. Refractive indices of thin films were expressed as a dispersion relation in a polynomial form, while extinction coefficients were modelled as a convolution by Lorentzian curves. It was observed that magnesium doping decreased the refractive index and also caused a blue shift in absorption edge which is a clear indicator of band gap widening.

Keywords: *Doping; refractive index; sol-gel; thin films; ZnO*

1. Introduction

Owing to its superior physical properties such as direct wide band gap of 3.37eV, high transparency in wide optical region, radiation hardness, and tunable conductivity ZnO is subjected to many studies (Look, 2001; Kang and Joung, 2007; Sennik et al., 2015). Researchers aim to benefit from ZnO in numerous fields such as gas sensors, lasers, field-effect transistors, and solar cells (Ozgur et al., 2005; Park et al., 2012; Sahin et al., 2014; Tulun et al., 2016; Ning et al., 2018; Zang, 2018).

Physical properties of ZnO can further be improved by various dopant materials. For this reason, implementation of various different elements into ZnO structure is widely studied. For instance, group IIA elements and among them especially magnesium doping to widen the band gap (Cao et al., 2013; Kim et al., 2014), aluminum to increase electrical conductivity (Tonbul et al., 2021), and yttrium to increase hardness (Kaya et al., 2018). Influence of copper doping into ZnO structure is studied by many researchers. Mhamdi et al. (2014) showed that 2 at. copper % doping greatly improves crystallinity of sprayed ZnO thin films. Suja et al. (2015) showed that copper doping introduces p-type conductivity to ZnO films, though this p-type conductivity is not stable and turns to n-type conductivity over time due to extrinsic defects.

ZnO is also a very important material for its catalytic properties. Due to its catalytic nature, ZnO is subjected to many studies in life sciences such as antibacterial activity and breath analysis. In their study, Alev et al. (2021) showed that copper doping increases density of point defects in ZnO structure and thus greatly enhances ethanol sensing properties of ZnO based nanorods. On the other hand, Yalcin et al. (2020) showed that 2% magnesium doping into ZnO structure greatly inhibits hemolytic activity while leading an advanced antibacterial property. Since antibacterial property is mainly driven by interaction between incoming electromagnetic wave and catalytic material, determination of optical constants of catalytic materials is crucial.

If ZnO based materials are to be used in devices with heterostructures that composed of layers of different materials

* Corresponding author.
E-mail address: dogan.akcan@eng.bau.edu.tr (D. Akcan).
https://doi.org/10.51753/flsrt.1120679 Author contributions
Received 24 May 2022; Accepted 21 September 2022
Available online 20 October 2022

that provides carrier or optical confinement such as LEDs and high electron mobility transistors (HEMTs), the most relevant parameters would be the band gaps of each layer and the valence- and conduction-band offsets between the individual layers (Janotti and Van de Walle, 2009). Hence, success of application of ZnO based materials relies on band-gap engineering. In light of these discussions, it is also crucial to investigate modulation of band-gaps of Cu doped ZnO thin films (ZnCuO) which can be achieved by introduction of magnesium into material. To the best of our knowledge, variation of these properties of ZnCuO films with magnesium doping has not yet been investigated.

In this study effect of magnesium doping on optical constants (refractive index and extinction coefficient) of $Zn_{0.98-x}Cu_{0.02}Mg_xO$ (x=0.0, 0.01, 0.02, 0.05, and 0.1) thin films were investigated. Optical constants were determined by application of Fresnel Equations to transmittance data numerically. Determined optical constants were then used determine the band gap variation of samples.

2. Materials and methods

The $Zn_{0.98-x}Cu_{0.02}Mg_xO$ thin films were deposited by sol-gel dip coating method with a varying magnesium molar ratio of $x = 0.0$ ($Zn_{0.98}Cu_{0.02}O$), 0.01, 0.02, 0.05, and 0.1. Zinc acetate dihydrate, magnesium acetate tetrahydrate, and copper (II) acetate monohydrate were used as precursors while Methanol was used as solvent and monoethanolamine (MEA) as sol stabilizer.

All chemicals were analytical grade and used as they were received from supplier (Merck). 0.25M precursor solution was prepared in solvent and MEA was added dropwise as precursors dissolved. MEA/total precursor molar ratio in solution was arranged as 1:1. Resultant solution was stirred in ambient conditions overnight to age. Soda-lime glass slides (ISOLAB) were used as substrate.

In order to coat the glass slides, slides were dipped into coating solution and withdrawn directly into vertical furnace. A preheat treatment was applied at 300°C for 2 minutes to remove organic materials, then coated substrate was cooled for 3 minutes. This process was repeated 20 times to achieve an appropriate thickness of thin films.

Film coated slides were finally annealed at 600°C to obtain crystalline structure. Shimadzu UV-mini 1240 spectrophotometer was used to measure optical transmittance of thin films.

3. Results and discussion

3.1. Transmittance measurements

As shown in Fig. 1 all films exhibit high transmittance in visible and NIR region. Besides slight fluctuation in transmittance due to interference caused by internal reflections, no other significant absorption troughs were observed. Average transmittance slightly decreased with low magnesium doping ratios of 1% and 2%, but further increase of magnesium doping ratio resulted with distinctive increase in blue region of spectrum.

While $Zn_{0.98}Cu_{0.02}O$ film exhibit a sharp optical cutting edge around 380 nm, cutting edge shifted towards shorter wavelengths with increasing magnesium doping. Detailed representation of this blue shift in cutting edge is shown as an inset in Fig. 1.

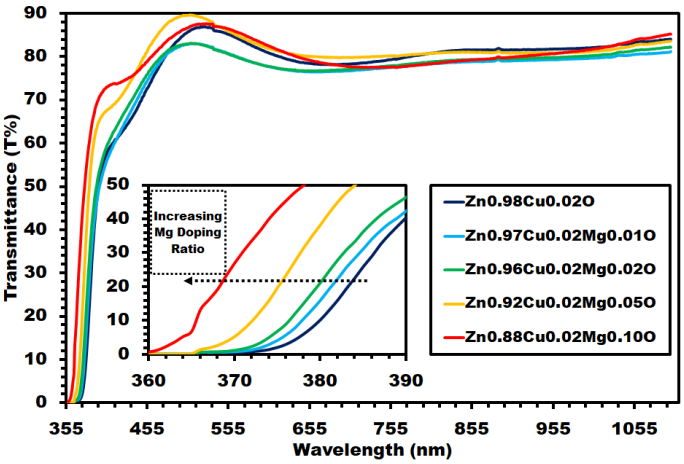

Fig. 1. Optical transmittance of the $Zn_{0.98-x}Cu_{0.02}Mg_xO$ thin films. Inset figure shows close up view of transmittance in 360-390 nm wavelength interval.

3.2. Determination of optical constants and modeling transmittance of films

Details of transmittance model of "Double Facet Coated Substrate" (DFCS) were discussed in an earlier study of our research group (Akcan et al., 2019). This transmittance model can be summarized as follows:

Coefficients of reflection and transmission of the electric field (r_{12} and t_{12}, respectively) from one medium to another with complex refractive indices (η_1 and η_2, respectively) at a normal incidence is given by:

$$r_{12} = \frac{\eta_1 - \eta_2}{\eta_1 + \eta_2} \quad \text{.....(1)}$$

$$t_{12} = \frac{2\eta_1}{\eta_1 + \eta_2} \quad \text{.....(2)}$$

Here complex refractive index η is defined as $\eta = n + ik$, where n is the refractive index and k is the extinction coefficient. Resultant transmitted electric field is infinite summation of coherent electric fields which is subjected to reflection from air-film and film-substrate interfaces and experience wavelength dependent phase shift which is given by $\theta = 4\pi\eta_{film}d_{film}/\lambda$. The resultant reflection and transmission coefficients of electric field for air-film-substrate system (r_{afs} and t_{afs}, respectively) are given by:

$$r_{afs} = \frac{r_{af} + r_{fs} \times exp(i\theta)}{1 + r_{af} \times r_{fs} \times exp(i\theta)} \quad \text{.....(3)}$$

$$t_{afs} = \frac{t_{af} \times t_{fs} \times exp(i\theta/2)}{1 + r_{af} \times r_{fs} \times exp(i\theta)} \quad \text{.....(4)}$$

Using these coefficients reflectance and transmittance in air-film-substrate direction can be calculated as:

$$R_{afs} = r_{afs} \times r^*_{afs} \quad \text{.....(5)}$$

$$T_{afs} = \frac{n_s}{n_a} \times t_{afs} \times t^*_{afs} \quad \text{.....(6)}$$

where r^*_{afs} and t^*_{afs} are complex conjugates of reflection and transmission coefficients, respectively. Considering absorption loss of the substrate, which is given by $U = \exp(-\alpha_{sub}d_{sub})$

where α_{sub} is absorption coefficient of substrate and d_{sub} is the substrate thickness (1.1mm), resultant transmittance DFCS system is given by:

$$T_{system} = \frac{T_{afs} \times T_{sfa} \times U}{1 - R_{sfa}^2 \times U^2} \quad \text{.....(7)}$$

Various models are proposed and widely used to model refractive index of a material. Some of them are rather complex but also works well even in high absorption conditions, such as Adachi-Forouhi-Drude model or Tauc-Lorentz model (Ferlauto et al., 2002; Latzel et al., 2015). On the other hand, simpler models such as Cauchy's model or Sellmeier's model work well in low absorption conditions (Sun and Kwok, 1999; Ozgur et al., 2005; Ozharar et al., 2016). Despite their limitations, all these models work in a large wavelength interval. In this study, inspired from series expansion of functions, refractive indices of thin films were modelled as a 6th degree polynomial. This method is advantageous as it is simple, possible to use in high absorption conditions, and more sensitive to subtle variations in refractive index, though it can only be used in narrow wavelength intervals, since interval of convergence is limited.

Extinction coefficients were modelled as summation of Lorentzian curves which is given by:

$$k_{film} = \frac{A}{1+\left(\frac{E-E_A}{\Delta E_A}\right)^2} + \frac{B}{1+\left(\frac{E-E_B}{\Delta E_B}\right)^2} + \frac{C}{1+\left(\frac{E-E_C}{\Delta E_C}\right)^2} \quad \text{.....(8)}$$

where A, B, and C are peak heights; E_A, E_B, and E_C are peak centers; and ΔE_A, ΔE_B, and ΔE_C are peak widths.

Curve fitting was performed in 360-1100 nm wavelength interval, and fitting was performed by using built in functions of MATLAB software. Calculated refractive index of thin films is shown in Fig. 2 and dispersion equations of refractive index model is given in Table 1. The calculated refractive index values are in accordance with the values in the literature (Baig et al., 2020; El Hamidi et al., 2021). As seen in the Fig. 2, refractive indices of films have a broad trend of decrease with increasing magnesium doping ratio. A similar trend was also observed by Yang et al. (2009) in Mg-doped ZnO thin films.

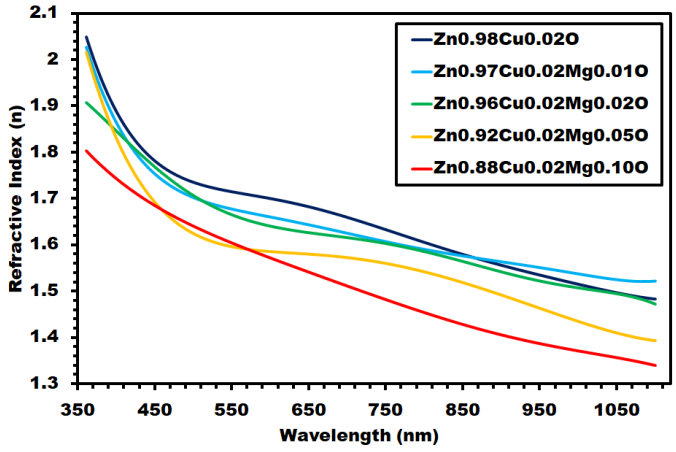

Fig. 2. Variation of refractive index of $Zn_{0.98-x}Cu_{0.02}Mg_xO$ thin films.

Calculated extinction coefficients of thin films are shown in Fig. 3. Intense absorption due to intrinsic band - gap in UV range can clearly be seen. Absorption edge shifts shorter wavelengths with increasing magnesium doping ratio which also was evident in transmittance graph [inset Fig. (3a)]. All films exhibit very low absorption in visible and NIR region. While there's no particular trend in variation of absorption in visible region, in NIR region absorbance was greatly increased with 1% doping but steadily decreased with further increase of magnesium doping, as shown in the inset Fig. (3b). Parameters of Lorentzian curves that constitute extinction coefficient are given in Table 2. Negative peak heights in $Zn_{0.93}Cu_{0.02}Mg_{0.05}O$ and $Zn_{0.88}Cu_{0.02}Mg_{0.10}O$ thin films do not have a physical significance. Since determination of extinction coefficient by summation of Lorentzian curves is an emprical method, "negative peaks" only act as a correction factor in their respective regions.

Besides refractive index and extinction coefficient, this model also enables determination of thickness of thin films. Evaluated thin film thicknesses are shared in Table 3.

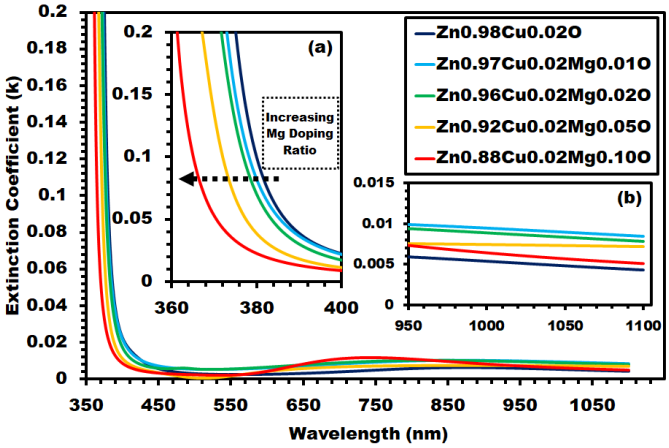

Fig. 3. Extinction coefficients of $Zn_{0.98-x}Cu_{0.02}Mg_xO$ thin films. Close up view of extinction coefficients in 360-400 nm and 950-1100 nm wavelength intervals were shown in inset figures (a) and (b) respectively.

Transmittance of thin films were modelled from calculated refractive index and extinction coefficient. Accuracy of transmittance model is determined from correlation coefficient R^2. As seen in the Fig. 4, transmittance model is highly accurate as R^2 values are very close to 1.

3.3. Determination of band gap

Energy gap or band gap (E_g) of a material is the energy required to excite an electron from the valence band to the conduction band. This energy gap obeys the relation which is given as

$$(\alpha h\nu)^n = A(h\nu - E_g) \quad \text{.....(9)}$$

Here α is absorption coefficient, h is Planck constant, ν is frequency of incoming light, A is proportionality constant, and E_g is band gap of the material. The exponent n get its value according to nature of electronic transition. Since ZnO is a direct band gap material, n is equal to 2. E_g can be estimated from extrapolating linear part of $h\nu$ vs. $(\alpha h\nu)^2$ graph which is also known as Tauc plot. Many studies evaluate α from Beer-Lambert law, which is given by (Scarminio et al., 1999; Za'Aba et al., 2014; Chen and Jaramillo, 2017).

$$I = I_0 e^{-\alpha t} \quad \text{.....(10)}$$

Table 1
Refractive index dispersion relations with varying Mg doping ratio.

Mg Doping Ratio (at.%)	Refractive index dispersion relation (Wavelength – λ – is given in μm)
0	$n_{Mg=0\%} = 70.014 \cdot \lambda^6 - 347.99 \cdot \lambda^5 + 710.5 \cdot \lambda^4 - 761.01 \cdot \lambda^3 + 449.96 \cdot \lambda^2 - 139.41 \cdot \lambda + 19.451$
1	$n_{Mg=1\%} = 86.40 \cdot \lambda^6 - 413.39 \cdot \lambda^5 + 813.52 \cdot \lambda^4 - 842.31 \cdot \lambda^3 + 483.87 \cdot \lambda^2 - 146.58 \cdot \lambda + 20.04$
2	$n_{Mg=2\%} = -81.16 \cdot \lambda^6 + 360.17 \cdot \lambda^5 - 644.25 \cdot \lambda^4 + 590.32 \cdot \lambda^3 - 289.08 \cdot \lambda^2 + 70.10 \cdot \lambda - 4.59$
5	$n_{Mg=5\%} = 35.01 \cdot \lambda^6 - 181.50 \cdot \lambda^5 + 393.94 \cdot \lambda^4 - 455.86 \cdot \lambda^3 + 294.56 \cdot \lambda^2 - 100.35 \cdot \lambda + 15.65$
10	$n_{Mg=10\%} = -1.67 \cdot \lambda^6 - 2.32 \cdot \lambda^5 + 24.79 \cdot \lambda^4 - 46.05 \cdot \lambda^3 + 37.91 \cdot \lambda^2 - 15.52 \cdot \lambda + 4.23$

Table 2
Lorentzian curve parameters of extinction coefficient.

Parameter	$Zn_{0.98}Cu_{0.02}O$	$Zn_{0.97}Cu_{0.02}Mg_{0.01}O$	$Zn_{0.96}Cu_{0.02}Mg_{0.02}O$	$Zn_{0.93}Cu_{0.02}Mg_{0.05}O$	$Zn_{0.88}Cu_{0.02}Mg_{0.10}O$
A	0.5181	2.0138	0.3386	0.2479	0.9114
B	0.0040	0.4137	0.0012	-0.0063	-0.0047
C	0.0059	0.0095	0.0098	0.0083	0.0129
E_A (eV)	3.3739	3.7479	3.3900	3.4073	3.5046
E_B (eV)	3.0115	3.3874	2.5583	2.3980	2.1336
E_C (eV)	1.4102	1.4146	1.4904	1.5790	1.7001
ΔE_A (eV)	0.0535	0.0322	0.0640	0.0597	0.0379
ΔE_B (eV)	0.1877	0.0571	0.1046	0.3652	0.2932
ΔE_C (eV)	0.4073	0.6320	0.6708	1.3946	0.4721

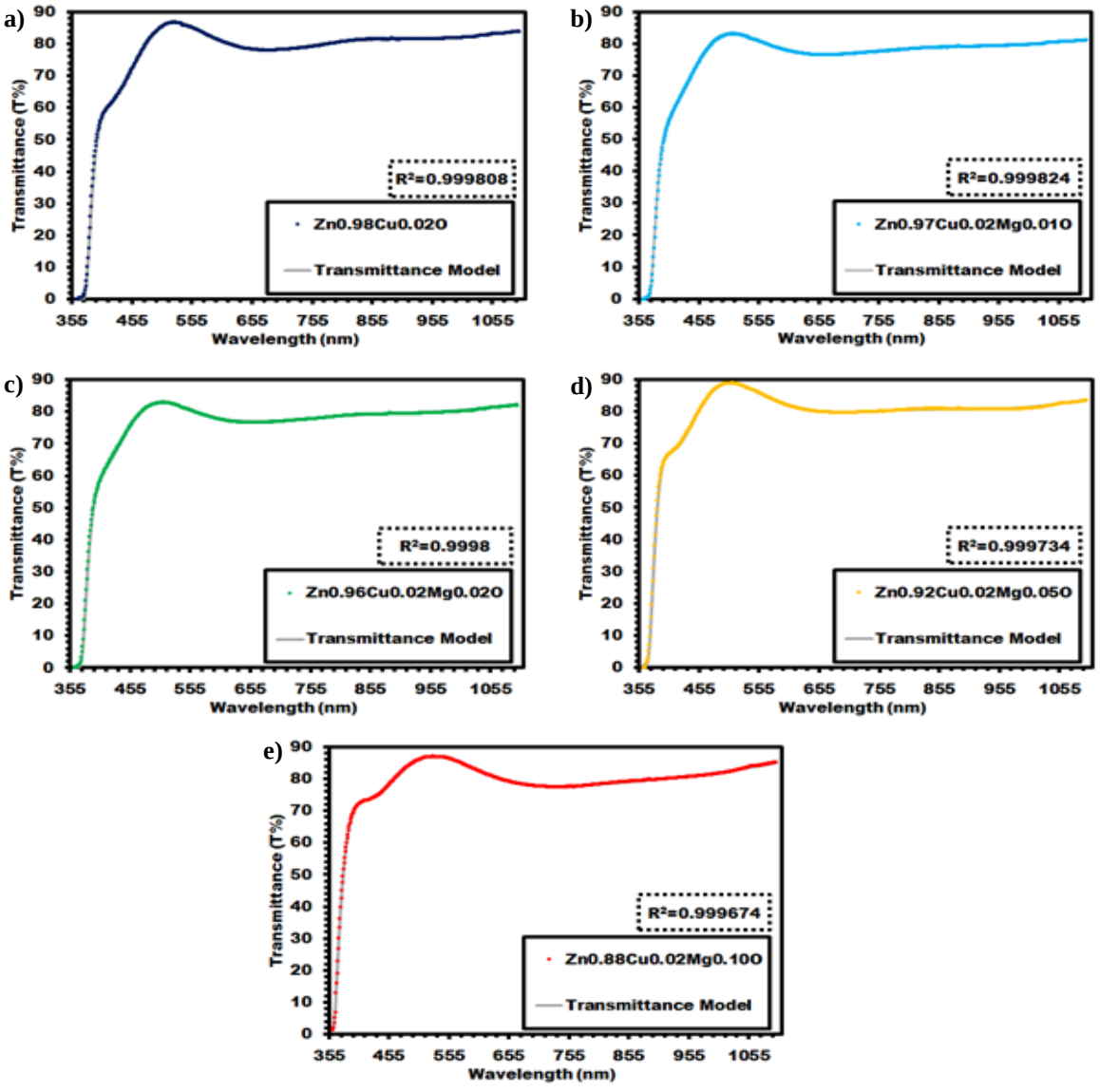

Fig. 4. Comparison of transmittance model with measurement results: (a) $Zn_{0.98}Cu_{0.02}O$, (b) $Zn_{0.97}Cu_{0.02}Mg_{0.01}O$, (c) $Zn_{0.96}Cu_{0.02}Mg_{0.02}O$, (d) $Zn_{0.92}Cu_{0.02}Mg_{0.05}O$, (e) $Zn_{0.88}Cu_{0.02}Mg_{0.10}O$.

where I is transmitted light intensity, I_0 is incoming light intensity and t is film thickness. In order to obtain α, considering $I/I_0 = 1/T$, equation (10) can be re-written as:

$$\alpha = \frac{-1}{t} \ln\left(\frac{1}{T}\right) \quad \text{.....(11)}$$

Table 3
Evaluated thicknesses of $Zn_{0.98-x}Cu_{0.02}Mg_xO$ thin films with transmittance model.

Mg Doping Ratio (at.%)	Film Thickness (nm)
0	302
1	295
2	290
5	305
10	320

where T is the transmittance of the sample. To be fair, this approach is very simple and gives a rough idea about value of the band gap of sample and allows to estimate the trends about modifications made in samples. However, considering Beer's Law only to calculate band gap leads to errors, since thin films have a finite thickness and light traveling through the film is subjected to multiple reflections and interferences. For this reason, the evaluated band gap value is slightly erroneous and the error is considerable for applications requiring band gap engineering. Band gap of $Zn_{0.98}Cu_{0.02}O$ thin film was calculated using this method as an example. Tauc plot of subjected sample can be seen in Fig. 5. Band gap of sample calculated with this method was $E_g = 3.227$eV. Considering theoretical band gap of ZnO, this value is slightly less than expected.

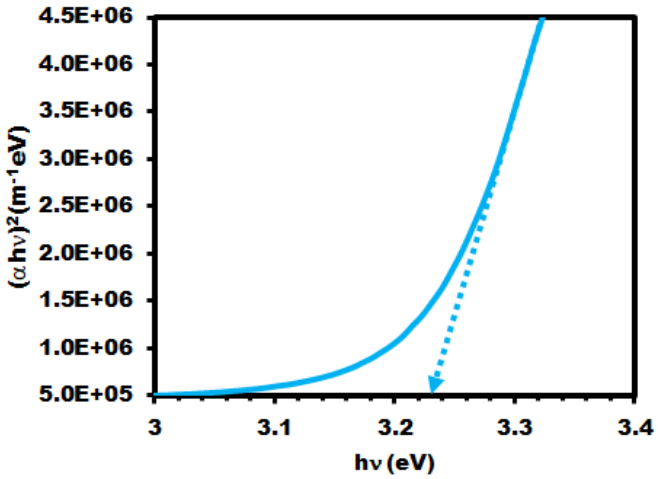

Fig. 5. Tauc plot of $Zn_{0.98}Cu_{0.02}O$ evaluated from Beer-Lambert Law.

Relation between extinction coefficient and absorption coefficient is given as:

$$\alpha = \frac{4\pi k}{\lambda} \quad \text{.....(12)}$$

In order to calculate band gaps of deposited films accurately, absorption coefficients of thin films were calculated from extinction coefficients which are evaluated from transmittance model.

Resultant Tauc plot of thin films is given in Fig. 6. As seen in the figure, magnesium doping leaded extrapolation to shift higher energies, which is a clear indicator of band gap widening.

As shown in the inset figure, evaluated band gap values has strong correlation with the relation $E_g = 0.0008x^2 + 0.0014x + 3.3147$, where x denotes for magnesium doping ratio. Evaluated band gap values are listed in Table 4. Comparison of band gap values of $Zn_{0.98}Cu_{0.02}O$ determined by different models shows that using Beer's law results 2.5% difference to the band gap calculated from transmittance model.

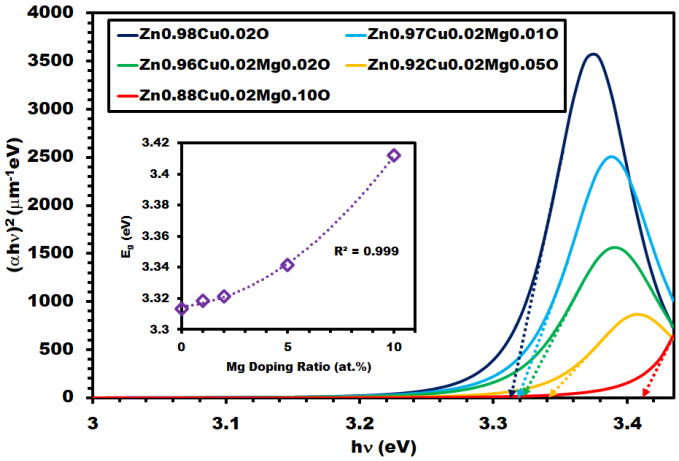

Fig. 6. Tauc plot of $Zn_{0.98-x}Cu_{0.02}Mg_xO$ thin films evaluated from transmittance model. Inset figure shows variation of band gap with increasing magnesium doping ratio.

Table 4
Evaluated band gap values of $Zn_{0.98-x}Cu_{0.02}Mg_xO$ thin films with transmittance model.

Mg Doping Ratio (at.%)	E_g (eV)
0	3.313
1	3.319
2	3.321
5	3.342
10	3.412

4. Conclusion

In conclusion; optical constants, namely refractive index and extinction coefficient of $Zn_{0.98-x}Cu_{0.02}Mg_xO$ thin films were calculated from experimental transmittance data numerically with a transmittance model relying on Fresnel equations. Refractive index is observed to be decreasing with increasing magnesium doping ratio. Absorption edge of thin films shifted towards higher energies, which is an indicator of band gap widening. Band gap values are calculated from extinction coefficients and a considerable increase is observed from 3.313eV to 3.412eV for 10 at % magnesium doped films.

This study has shown that Mg increases the band gap in exchange for lowering the refractive index. These results have great importance in development of new and improved antibacterial and sensing materials.

Acknowledgement: The presented work was supported by the Research Fund of Bahçeşehir University, Istanbul, Turkey (Project No. BAUBAP.2018.02.16).

Conflict of interest: The author declares that he has no conflict of interests.

Informed consent: The author declares that this manuscript did not involve human or animal participants and informed consent was not collected.

References

Akcan, D., Ozharar, S., Ozugurlu, E., & Arda, L. (2019). The effects of Co/Cu Co-doped ZnO thin films: An optical study. *Journal of Alloys and Compounds*, *797*, 253-261.

Alev, O., Ergun, I., Oezdemir, O., Arslan, L. C., Buyukkose, S., & Ozturk, Z. Z. (2021). Enhanced ethanol sensing performance of Cu-doped ZnO nanorods. *Materials Science in Semiconductor Processing*, *136*, 106149.

Baig, F., Ashraf, M. W., Asif, A., & Imran, M. (2020). A comparative analysis for effects of solvents on optical properties of Mg doped ZnO thin films for optoelectronic applications. *Optik*, *208*, 164534.

Cao, L., Zhu, L., & Ye, Z. (2013). Enhancement of p-type conduction in Ag-doped ZnO thin films via Mg alloying: The role of oxygen vacancy. *Journal of Physics and Chemistry of Solids*, *74*(5), 668-672.

Chen, Z., & Jaramillo, T. (2017). The Use of UV-Visible Spectroscopy to Measure the Band Gap of a Semiconductor. https://mmrc.caltech.edu/CaryUV-Vis Int.Sphere/Literature/ Spectroscopy Jaramillo.pdf, Last accessed on July, 2022.

El Hamidi, A., El Mahboub, E., Meziane, K., El Hichou, A., & Almaggoussi, A. (2021). The effect of electronegativity on optical properties of Mg doped ZnO. *Optik*, *241*, 167070.

Ferlauto, A. S., Ferreira, G. M., Pearce, J. M., Wronski, C. R., Collins, R. W., Deng, X., & Ganguly, G. (2002). Analytical model for the optical functions of amorphous semiconductors from the near-infrared to ultraviolet: Applications in thin film photovoltaics. *Journal of Applied Physics*, *92*(5), 2424-2436.

Janotti, A., & Van de Walle, C. G. (2009). Fundamentals of zinc oxide as a semiconductor. *Reports on Progress in Physics*, *72*(12), 126501.

Kang, S. J., & Joung, Y. H. (2007). Influence of substrate temperature on the optical and piezoelectric properties of ZnO thin films deposited by rf magnetron sputtering. *Applied Surface Science*, *253*(17), 7330-7335.

Kaya, S., Akcan, D., Ozturk, O., & Arda, L. (2018). Enhanced mechanical properties of yttrium doped ZnO nanoparticles as determined by instrumented indentation technique. *Ceramics International*, *44*(9), 10306-10314.

Kim, I. Y., Shin, S. W., Gang, M. G., Lee, S. H., Gurav, K. V., Patil, P. S., ... & Kim, J. H. (2014). Comparative study of quaternary Mg and Group III element co-doped ZnO thin films with transparent conductive characteristics. *Thin Solid Films*, *570*, 321-325.

Latzel, M., Gobelt, M., Bronstrup, G., Venzago, C., Schmitt, S. W., Sarau, G., & Christiansen, S. H. (2015). Modeling the dielectric function of degenerately doped ZnO: Al thin films grown by ALD using physical parameters. *Optical Materials Express*, *5*(9), 1979-1990.

Look, D. C. (2001). Recent advances in ZnO materials and devices. *Materials Science and Engineering: B*, *80*(1-3), 383-387.

Mhamdi, A., Mimouni, R., Amlouk, A., Amlouk, M., & Belgacem, S. (2014). Study of copper doping effects on structural, optical and electrical properties of sprayed ZnO thin films. *Journal of Alloys and Compounds*, *610*, 250-257.

Ning, Y., Zhang, Z., Teng, F., & Fang, X. (2018). Novel transparent and self-powered UV photodetector based on crossed ZnO nanofiber array homojunction. *Small*, *14*(13), 1703754.

Ozgur, U., Alivov, Y. I., Liu, C., Teke, A., Reshchikov, M., Dogan, S., Avrutin, V., Cho, S.-J., Morkoc, A. H. (2005). A comprehensive review of ZnO materials and devices. *Journal of Applied Physics*, *98*(4), 11.

Park, S. Y., Kim, B. J., Kim, K., Kang, M. S., Lim, K. H., Lee, T. I., Myoung, J.M., Hong Koo Baik Kim, Y. S. (2012). Low-temperature, solution-processed and alkali metal doped ZnO for high-performance thin-film transistors. *Advanced Materials*, *24*(6), 834-838.

Ozharar, S., Akcan, D., & Arda, L. (2016). Determination of the refractive index and the thickness of double side coated thin films. *Journal of Optoelectronics and Advanced Materials*, *18*(January-February 2016), 65-69.

Sahin, Y., Ozturk, S., Kilinc, N., Kosemen, A., Erkovan, M., & Ozturk, Z. Z. (2014). Electrical conduction and NO2 gas sensing properties of ZnO nanorods. *Applied Surface Science*, *303*, 90-96.

Scarminio, J., Urbano, A., & Gardes, B. (1999). The Beer-Lambert law for electrochromic tungsten oxide thin films. *Materials Chemistry and Physics*, *61*(2), 143-146.

Sennik, E., Kerli, S., Alver, U., & Ozturk, Z. Z. (2015). Effect of fluorine doping on the NO2-sensing properties of ZnO thin films. *Sensors and Actuators B: Chemical*, *216*, 49-56.

Suja, M., Bashar, S. B., Morshed, M. M., & Liu, J. (2015). Realization of Cu-doped p-type ZnO thin films by molecular beam epitaxy. *ACS Applied Materials & Interfaces*, *7*(16), 8894-8899.

Sun, X. W., & Kwok, H. S. (1999). Optical properties of epitaxially grown zinc oxide films on sapphire by pulsed laser deposition. *Journal of Applied Physics*, *86*(1), 408-411.

Tonbul, B., Can, H. A., Ozturk, T., & Akyildiz, H. (2021). Solution processed aluminum-doped ZnO thin films for transparent heater applications. *Materials Science in Semiconductor Processing*, *127*, 105735.

Tulun, F. R., Ozturk, S., & Ozturk, Z. Z. (2016). The NO_2 sensing properties of the sensors done with nano-tetrapods. *Acta Physica Polonica A*, *129*(4), 797-799.

Yalcin, B., Akcan, D., Yalcin, I. E., Alphan, M. C., Senturk, K., Ozyigit, I. I., & Arda, L. (2020). Effect of Mg doping on morphology, photocatalytic activity and related biological properties of $Zn_{1-x}Mg_xO$ nanoparticles. *Turkish Journal of Chemistry*, *44*(4), 1177-1199.

Yang, S., Liu, Y., Zhang, Y., & Mo, D. (2009). Spectroscopic ellipsometry studies of Mg-doped ZnO thin films prepared by the sol-gel method. *Physica Status Solidi (A)*, *206*(7), 1488-1493.

Za'Aba, N. K., Sarjidan, M. M., Majid, W. A., Kusrini, E., & Saleh, M. I. (2014). Junction properties and conduction mechanism of new terbium complexes with triethylene glycol ligand for potential application in organic electronic device. *Journal of Rare Earths*, *32*(7), 633-640.

Zang, Z. (2018). Efficiency enhancement of ZnO/Cu_2O solar cells with well oriented and micrometer grain sized Cu_2O films. *Applied Physics Letters*, *112*(4), 042106.

Cite as: Akcan, D. (2022). Determination of optical constants and band gap variation of $Zn_{0.98-x}Cu_{0.02}Mg_xO$ thin films. *Front Life Sci RT*, *3*(3), 101-106.